frontiers in Marine Science

ORIGINAL RESEARCH
published: 15 December 2021
doi: 10.3389/fmars.2021.741143

Water Exchange Between the Gulf of Ob and the Kara Sea During Ice-Free Seasons: The Roles of River Discharge and Wind Forcing

Alexander Osadchiev[1,2], Olga Konovalova[3] and Alexandra Gordey[1,2]*

[1] Shirshov Institute of Oceanology, Russian Academy of Sciences, Moscow, Russia, [2] Moscow Institute of Physics and Technology, Dolgoprudny, Russia, [3] Marine Research Center at Lomonosov Moscow State University, Moscow, Russia

OPEN ACCESS

Edited by:
Anas Ghadouani,
University of Western Australia,
Australia

Reviewed by:
Adam Ayouche,
Laboratoire de Physique des Océans et de Télédétection par Satellite (LOPS), France
Hans Burchard,
Leibniz Institute for Baltic Sea Research (LG), Germany
Heqin Cheng,
East China Normal University, China
Nils Edvin Asp,
Federal University of Pará, Brazil

***Correspondence:**
Alexander Osadchiev
osadchiev@ocean.ru

Specialty section:
This article was submitted to Coastal Ocean Processes, a section of the journal Frontiers in Marine Science

Received: 14 July 2021
Accepted: 12 November 2021
Published: 15 December 2021

Citation:
Osadchiev A, Konovalova O and Gordey A (2021) Water Exchange Between the Gulf of Ob and the Kara Sea During Ice-Free Seasons: The Roles of River Discharge and Wind Forcing. Front. Mar. Sci. 8:741143. doi: 10.3389/fmars.2021.741143

The Gulf of Ob is among the largest estuaries in the World Ocean in terms of area, watershed basin, and freshwater discharge. In this work, we describe the roles of river discharge and wind forcing on the water exchange between the Gulf of Ob and the Kara Sea during ice-free seasons. This work is based on the extensive *in situ* measurements performed during 10 oceanographic surveys in 2007–2019. Due to large river runoff (∼530 km^3 annually) and low tidal forcing (<0.5 m/s), the estuarine processes in the Gulf of Ob during the ice-free season are generally governed by gravitational circulation. Local wind forcing significantly affects general estuarine circulation and mixing only in rare cases of strong winds (∼10 m/s). On the other hand, remote wind forcing over the central part of the Kara Sea regularly intensifies estuarine—sea water exchange. Eastern winds in the central part of the Kara Sea induce upwelling in the area adjacent to the Gulf of Ob, which increases the barotropic pressure gradient between the gulf and the open sea. As a result, intense and distant (120–170 km) inflows of saline water to the gulf occur as compared to the average conditions (50–70 km). Remote wind forcing has a far stronger impact on saltwater intrusion into the Gulf of Ob than the highly variable river discharge rate. In particular, saltwater reaches the shallow central part of the gulf only during upwelling-induced intense inflows. In the other periods (even under low discharge conditions), fresh river water occupies this area from surface to bottom. The upwelling-induced intense inflows occur on average during a quarter of days (July to October) when the gulf is free of ice. They substantially increase the productivity of phytoplankton communities in the gulf and modify the taxa ratio toward the increase of brackish water species and the decrease of freshwater species.

Keywords: estuarine circulation, salt-wedge estuary, remote upwelling, stratification, phytoplankton communities, Gulf of Ob, Kara Sea

INTRODUCTION

The Gulf of Ob is located in the southern part of the Kara Sea and is among the largest river estuaries in the World Ocean (**Figure 1**). The Gulf of Ob is long (850 km) and narrow (30–80 km), and its area is about 41,000 km^2, while the area of its watershed basin is 3,320,000 km^2 (∼2.2% of Earth's land). The Gulf of Ob receives approximately 530 km^3 (16,800 m^3/s on average) of freshwater discharge annually, namely, 430 km^3 (13,600 m^3/s) from the Ob River and 100 km^3 (3,200 m^3/s) from the Taz River, the Pur River, and smaller rivers (Gordeev et al., 1996; Pavlov et al., 1996). This large freshwater volume accounts for ~15% of the total freshwater runoff to the Arctic Ocean (Guay et al., 2001) and ~1.5% of the total freshwater runoff to the World Ocean (Oki and Kanae, 2006).

The majority of runoff from the rivers inflowing to the Gulf of Ob is provided during the flooding period from May to September (Pavlov et al., 1996). Maximal discharge to the gulf is registered at the end of May and is induced by ice melting in the watershed area of the gulf (**Figure 1C**). However, the decrease of river runoff usually is very slight till the end of September. For certain years, discharge during the secondary rain-induced peak can be the same or higher in the beginning of September than in May (Osadchiev et al., 2021a).

The rivers inflowing to the gulf are frozen from November to May, which result in a relatively low discharge rate in winter and spring (2,000–5,000 m^3/s) (**Figure 1C**). The Gulf of Ob is covered by ice from October to November till May to June, and the water temperature of the surface layer during this period is 0°C. The average temperature of the surface layer in July and September is 2–3°C, while in August it increases up to 8°C (Gladysh et al., 2017). Tidal circulation in the gulf is dominated by the semidiurnal tide (Kagan et al., 2010). Tidal amplitudes during the ice-free periods are 100–140 cm in the northern part of the Gulf of Ob, and they decrease to 60–80 cm in the central part of the gulf and to 20–50 cm in the southern part of the gulf (Voinov, 2016).

River water occupies the whole water column in the southern and central part of the Gulf of Ob during ice-free periods. The northern part of the gulf is a typical salt-wedge estuary with a large salinity gradient between the freshened surface layer and the saline bottom layer formed by water inflow from the Kara Sea. The location of the frontal zone between freshwater and saline water in the bottom layer shows distinct seasonal variability governed by large seasonal variability of the river discharge rate (Lapin, 2011; Lapin et al., 2015), which is a common feature of river estuaries (Hansen and Rattray, 1965; Moller et al., 2001; Chawla et al., 2008; Miranda et al., 2017).

In this study, we demonstrate that wind forcing can strongly modify the estuarine—ocean exchange in the Gulf of Ob in particular that can exceed the role of seasonal variability of the river discharge rate. In contrast to typical shallow estuaries, this process is induced by remote wind forcing, while local winds limitedly affect the general circulation in the gulf. Based on *in situ* salinity measurements performed during 10 different oceanographic surveys in the Gulf of Ob in 2007–2019 and satellite observations, we show that upwelling events in the central part of the Kara Sea adjacent to the Gulf of Ob induce intense and distant inflows of saline seawater to the gulf. We focus on *in situ* measurements performed in the Gulf of Ob in August 2019, which revealed the most intense and distant inflow of saline seawater into the gulf, and demonstrate that these intense inflows of saline water to the gulf significantly affect qualitative and quantitative characteristics of the local phytoplankton communities.

The paper is organized as follows. Section 2 provides the detailed information about the *in situ*, satellite, river discharge, and wind forcing data used in this study. The relation between the external forcing conditions and the intensity of inflow of saline seawater to the gulf is described in Section 3 with an emphasis on the intense inflow registered in August 2019. The influence of inflows of saline water on the biological structure of the gulf, as well as the assessment of its variability on synoptic, seasonal, and inter-annual time scales, is analyzed and discussed in Section 4, followed by conclusions in Section 5.

DATA AND METHODS

The salinity *in situ* data used in this study were collected during 10 oceanographic surveys in the Gulf of Ob in September 2007, August and September 2010, September 2013, August and September 2014, July 2016, and July and August 2019 (Lapin, 2011; Lapin et al., 2015; Drits et al., 2016, 2017; Borisenko et al., 2021; Osadchiev et al., 2021a; **Table 1** and **Figure 2**). The vertical salinity structure was measured at the hydrographic stations in the northern and central part of the Gulf of Ob using a CTD instrument (*SBE 911plus*) at 0.2-m spatial resolution. Based on these measurements, we reconstructed the locations of the isohaline of five in the bottom layer of the Gulf of Ob (**Table 1**, arrows in **Figure 2**). This value is indicative of the intensity of an inflow of saline seawater to the Gulf of Ob and is analyzed in this study.

Biological *in situ* data used in this study were collected during the three oceanographic surveys in the Gulf of Ob in September 2007, September 2014, and August 2019 (Sukhanova et al., 2010; Flint and Poyarkov, 2015; Flint et al., 2020; **Table 1**). In these surveys, qualitative (list of species and abundance of taxa) and quantitative (total abundance and biomass) characteristics were registered at the selected stations. Water sampling was performed with Niskin bottles from surface, halocline, and bottom layers. The water probes were concentrated and preserved in phormamide or Lugol's iodine solution. Measurements were performed using light microscopes. Phytoplankton abundance was registered by calculating the cells in Najott (10^{-5} L) and Fuchs–Rosenthal (3.2×10^{-6} L) chambers three times for each sample. The biomass of microalgae was calculated from cell volume using the method of geometric similarity of figures (Hillebrand et al., 1999).

The wind forcing conditions in this study area were examined using *in situ* measurements at the meteorological station of Seyakha located in the central part of the Gulf of Ob (indicated by the red circle in **Figure 1**) and the ERA5 atmospheric reanalysis with a 0.25° spatial and hourly temporal resolution (Hersbach et al., 2020). To evaluate the influence of wind forcing on estuarine circulation, we calculated the four time integrals of wind stress $W = \int \tau \times dt$ during the periods of downwelling (western wind, $\tau_x > 0$), upwelling (eastern wind, $\tau_x < 0$), offshore (southern wind, $\tau_y > 0$), and onshore (northern wind, $\tau_y < 0$) wind forcing. In particular, the upwelling integral of wind stress W_u is the result of integration of zonal wind stress τ_x only during the periods when $\tau_x < 0$.

The discharge data used in this study were obtained at the most downstream gauge station on the Ob River in Salekhard,

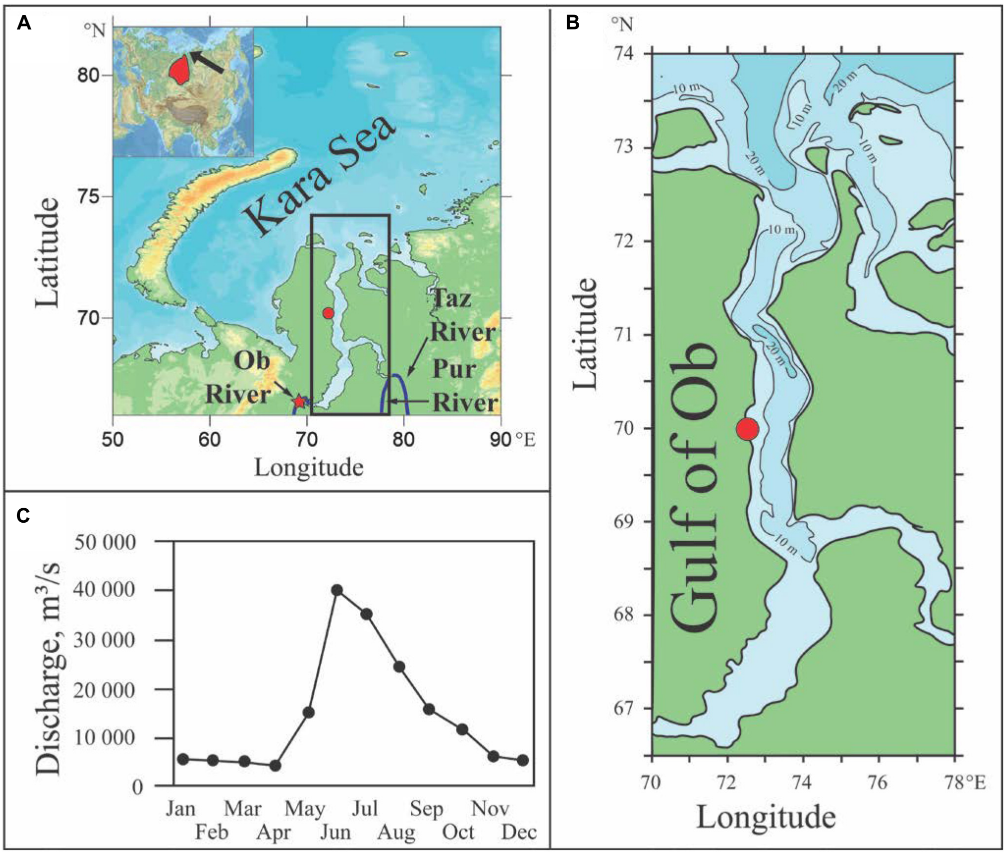

FIGURE 1 | Location of the Gulf of Ob (indicated by the black box) in the Kara Sea (the black arrow at the inset); the main rivers inflowing to the Gulf of Ob; the gauge station in Salekhard (the red star) and the meteorological station in Seyakha (the red circle); the watershed area of the Gulf of Ob shown at the Eurasian map (the red area at the inset) **(A)**; bathymetry of the Gulf of Ob **(B)**; and mean annual hydrograph of the Ob, Pur, and Taz rivers **(C)**.

which is located at the southern edge of the Gulf of Ob (indicated by the red star in **Figure 1**). In this study, we address the processes in the central and northern part of the gulf; therefore, we have to analyze the timing of runoff entering this region. The distance between Salekhard and the study area is ~750 km. Therefore, we shifted the hydrograph measured in Salekhard by 30 days onward according to estimates of the average flow speed in the Gulf of Ob and Yenisei gulfs (0.3 m/s; Harms and Karcher, 1999).

Satellite data used in this study include Sentinel-2 optical imagery, MODIS optical imagery and thermal data, and AVISO altimetry data.

RESULTS

Gravitational, Tidal, and Wind Forcing in the Gulf of Ob

The Gulf of Ob is a classical positive estuary with a general seaward transport of freshened riverine water in the surface layer and a landward transport of saline seawater in the bottom layer. During the ice-free season, salinity in the Gulf of Ob is equal to 0 from surface to bottom in the shallow (<10 m) southern and central part of the estuary. Further northward, in the northern part of the gulf, the river flow detaches from the bottom and forms a freshened surface layer with depth ~10 m (Lapin, 2011; Osadchiev et al., 2021a). Surface salinity steadily increases within the northern part of the gulf and is equal to 4–10 when it outflows to the open sea (Osadchiev et al., 2021a). Salinity of the bottom layer within the northernmost part of the gulf is 30–32 and decreases landward.

Circulation and mixing in river estuaries generally are governed by gravitational forcing (due to salinity difference in river water and seawater), tidal forcing, and wind forcing. The relatively shallow Gulf of Ob receives very large freshwater discharge, which results in strong longitudinal density gradient (Osadchiev et al., 2021a). On the opposite, tidal circulation in the gulf is relatively low, the maximal tidal velocities are 0.4–0.5 m/s (Pavlov et al., 1996; Vvedensky et al., 2017). In the absence of wind forcing, the estuarine dynamical and mixing regime determined by the buoyancy and tidal forcing can be characterized by two dimensionless parameters, namely, the freshwater Froude number $Fr_f = \frac{U_R}{\sqrt{\beta g S H}}$ and the mixing parameter $M = \frac{C_D U_T^2}{w N_0 H^2}$, where U_R is the inflowing river velocity, U_T is the amplitude of the depth-averaged estuarine tidal velocity, w is the estuarine

TABLE 1 | Periods, research vessels, and locations of the isohaline of five in the bottom layer during 10 oceanographic surveys in 2007–2019.

Period	Research vessel	Data reference	Location of the isohaline of 5 in the bottom layer
23-25.09.2007	Akademik Mstislav Keldysh	Sukhanova et al., 2010; Osadchiev et al., 2021a	72.1°N
5-9.08.2010	OTA-777	Lapin, 2011	72.1°N
23-26.09.2010	OTA-777	Lapin, 2011	72.0°N
3-5.09.2013	Professor Shtokman	Drits et al., 2017	71.6°N
16-20.08.2014	Professor Shtokman	Flint and Poyarkov, 2015; Osadchiev et al., 2021a	72.3°N
13-21.09.2014	Briz	This paper (biology) Lapin et al., 2015	72.3°N
18-20.07.2016	Akademik Mstislav Keldysh	Sukhanova et al., 2018; Osadchiev et al., 2021a	71.6°N
16-18.07.2019	Akademik Mstislav Keldysh	Flint et al., 2020; Borisenko et al., 2021	72.1°N
8-10.08.2019	Kartesh	This paper (hydrology)	71.7°N
18-20.08.2019	Kartesh	This paper (biology and hydrology)	71.0°N

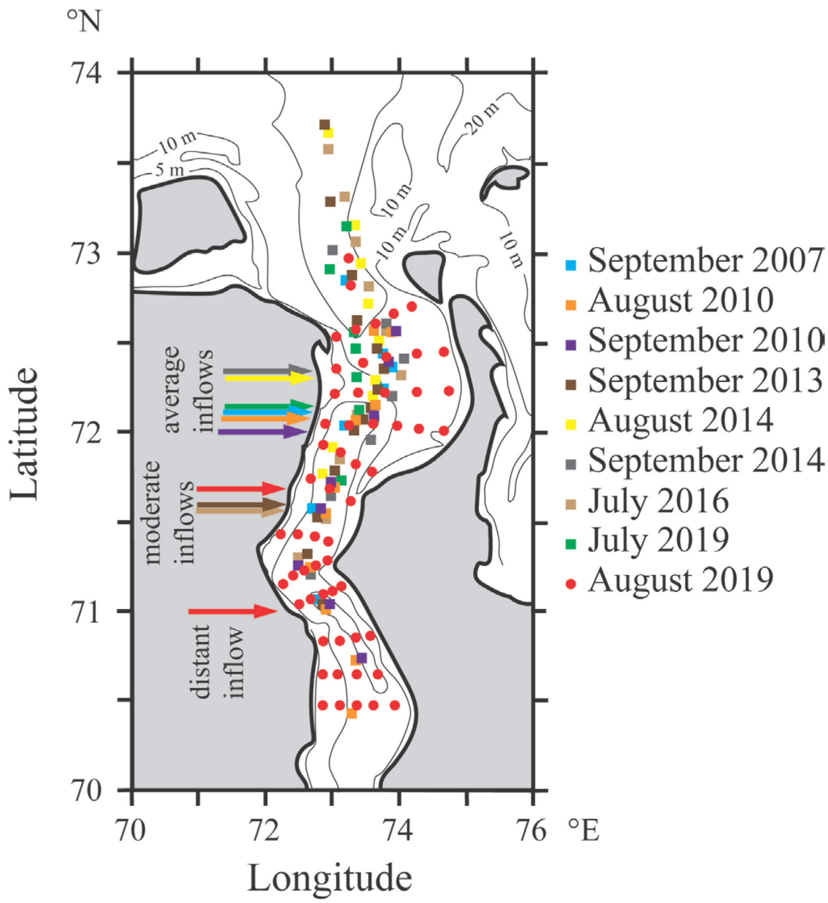

FIGURE 2 | Hydrographic stations of 10 oceanographic field surveys conducted in the Gulf of Ob in 2007–2019 (circles for the two surveys in August 2019, squares for all other cruises). Arrows indicate southernmost detected locations of the isohaline of five in the bottom layer of the Gulf of Ob. Note that the two surveys in August 2019 are indicated by two red arrows.

tidal frequency, S is the ambient sea salinity, H is the depth of an estuary, g is the gravity acceleration, β is the saline contraction coefficient prescribed equal to 7.7×10^{-4}, C_D is the quadratic drag coefficient for wind stress parameterization prescribed equal to 10^{-3}, and $N_0 = \sqrt{\frac{\beta g S}{H}}$ is the buoyancy frequency for maximum top-to-bottom salinity variation in an estuary (Geyer and MacCready, 2014). Values of these parameters for the Gulf of Ob are as follows: $Fr_f \sim 0.3/(7.7 \times 10^{-4} \times 10 \times 32 \times 15)^{0.5} \sim 0.6$, $M \sim 10^{-3} \times (0.4)^2/[2.3 \times 10^{-5} \times (7.7 \times 10^{-4} \times 10 \times 32/15)^{0.5} \times (15)^2] \sim 0.4$. The obtained estimations demonstrate that the Gulf of Ob is a typical salt-wedge estuary with strong vertical stratification due to very large freshwater runoff during the ice-free season, while tidal forcing limitedly affects circulation and mixing in the gulf.

The influence of wind forcing on the estuarine processes in the Gulf of Ob was assessed using the dimensionless Wedderburn number $We = \frac{\tau L}{\Delta \rho g H^2}$, where τ is the along-estuary wind stress, L is the length of the considered segment of the estuary, and $\Delta\rho$ is the density difference over L (Monismith, 1986; Chen and Sanford, 2009; Lange and Burchard, 2019). Once the along-estuary wind speed is large enough so that $We \sim 1$, the role of wind forcing is comparable with the role of gravitational circulation (Geyer, 1997; Chen and Sanford, 2009; Lange and Burchard, 2019; Lange et al., 2020). In case of the northern part of the Gulf of Ob with a two-layer stratification induced by saline inflows, $We \sim \tau \times 150 \times 10^3/6 \times 10 \times (20)^2 = \tau \times 6.25$. According to *in situ* measurements of wind forcing at the meteorological station of Seyakha, the average monthly wind speed in the study area from July to October in 2005–2020 varies between 5.5 and 5.7 m/s, while the maximal registered wind speed is 20 m/s. No prevailing wind direction is registered during the warm period; the repeatability of all eight compass wind directions is 10–15%. Therefore, for the study area we consider the average along-estuary wind speed equal to 5 m/s. In this case, $We \sim 0.04 \times 6.25 = 0.25$, which shows that under average wind forcing the estuarine circulation is governed mainly by gravitational circulation.

Local wind forcing affects estuarine circulation and mixing in case of strong along-estuary wind speed ~10 m/s because in this case $We \sim 0.16 \times 6.25 = 1$. In particular, strong up-estuary wind is expected to intensify estuarine circulation and increase stratification, while strong down-estuary wind tends to induce wind straining (Chen and Sanford, 2009; Lange and Burchard, 2019). Indeed, Osadchiev and Sedakov (2019) reported that strong northern winds reverse surface flow in the northwestern part of the gulf, i.e., change its predominant flow direction from northward to southward. However, the along-estuary wind speed exceeds 10 m/s during only 4% of days during the ice-free season; therefore, the local wind forcing significantly modifies general circulation and mixing in the Gulf of Ob only in rare cases.

While showing no modification in general estuarine circulation, moderate local wind forcing has a certain influence on circulation in the surface layer in the northern part of the Gulf of Ob during ice-free periods, which can be detected at optical satellite imagery (**Figure 3**). The general northward flow is observed within the southern and central part of the gulf occupied by fresh river water from surface to bottom. Circulation in the deeper and wider northern part of the gulf is more complex. According to the coastline and local bathymetry, riverine water propagates northward in this part of the gulf along its western shore as a narrow stream (10–25 km wide) (illustrated by solid black arrows in **Figure 3b**). Inflows of more saline water from the open sea to the northern part of the gulf occur along its eastern shore (illustrated by dashed black arrows in **Figure 3b**). Note that the estuarine—sea salinity difference is only several units of salinity, which is by an order of magnitude smaller than the salinity difference between the surface and bottom layer at this area. The anticyclonic circulation pattern is distinctly observed during moderate southern and eastern winds (**Figures 3a–d**). Northern and western winds, on the opposite, hamper the anticyclonic circulation and cause the formation of multiple mesoscale eddies and complex frontal zones at the periphery of the riverine stream and in the northeastern part of the gulf (**Figures 3e,f**). However, the influence of local wind forcing on the mesoscale structure of surface circulation in this area requires additional study.

Seawater Inflows to the Gulf of Ob

The intensity of inflow of saline seawater to the Gulf of Ob (indicated by the location of the isohaline of five in the bottom layer) shows large variability during the considered field surveys (**Table 1** and **Figures 2**, **4**). In most cases, saline seawater reached the latitude of 72.0–72.3°N (**Figure 4A**). More distant inflow (i.e., distant from the open sea) was observed in September 2013 and July 2016 (71.6°N) (hereafter referred to as "moderate inflows") (**Figure 4B**); the most distant inflow was registered in August 2019 (71.0°N) (hereafter referred to as "intense inflow"). Moreover, this distant inflow was observed in progress, on August 8–10, 2019 saline water was registered at the latitude of 71.7°N (**Figure 4C**), and 10 days later it reached 71.0°N (**Figure 4D**).

Previous studies of this process by Lapin (2011) and Lapin et al. (2015) based on three field surveys (August 2010, September 2010, and September 2014) reported significantly smaller variability of the salt-water intrusion to the gulf (72.0–72.3°N) and its association with the seasonal variability of river discharge. However, an analysis of more extensive *in situ* data demonstrates no direct dependence between the intensity of seawater inflow and the river discharge rate, including both instant discharge (**Figure 5A**) and average discharge rates from the beginning of summer freshet till the periods of oceanographic field surveys (**Figure 5B**).

The distances of seawater propagation to the gulf among different years with similar discharge conditions varied by ~50 km in July (light brown and green squares in **Figure 5**), ~150 km in August (yellow square and red circles), and ~70 km in September (dark brown and gray squares). On the other hand, similar inflow distances (72.1°N) were registered in July 2019 (green square in **Figure 5**), August 2010 (orange square), and September 2007 (cyan square) with significantly different discharge conditions. Finally, two of the three cases with distant inflows of saline water to the gulf, namely, a moderate inflow in July 2016 (light brown square in **Figure 5**) and an intense inflow in August 2019 (red circles), were registered during high discharge conditions (25,000–30,000 m^3/s). The moderate inflow in September 2013 (dark brown square in **Figure 5**), however, occurred during the drought period (11,000 m^3/s) of the year with relatively low annual runoff. The correlation coefficient between the inflow intensity and river discharge is −0.1 (**Figure 6A**), and the correlation coefficient between the inflow intensity and average discharge from the beginning of summer freshet till the periods of oceanographic field surveys is 0.

As discussed earlier, local winds limitedly affect the circulation in the bottom layer due to strong gravitational forcing and vertical stratification in the northern part of the Gulf of Ob. The saline inflow distances also do not show any dependence on the along-estuary wind stress, and the related correlation

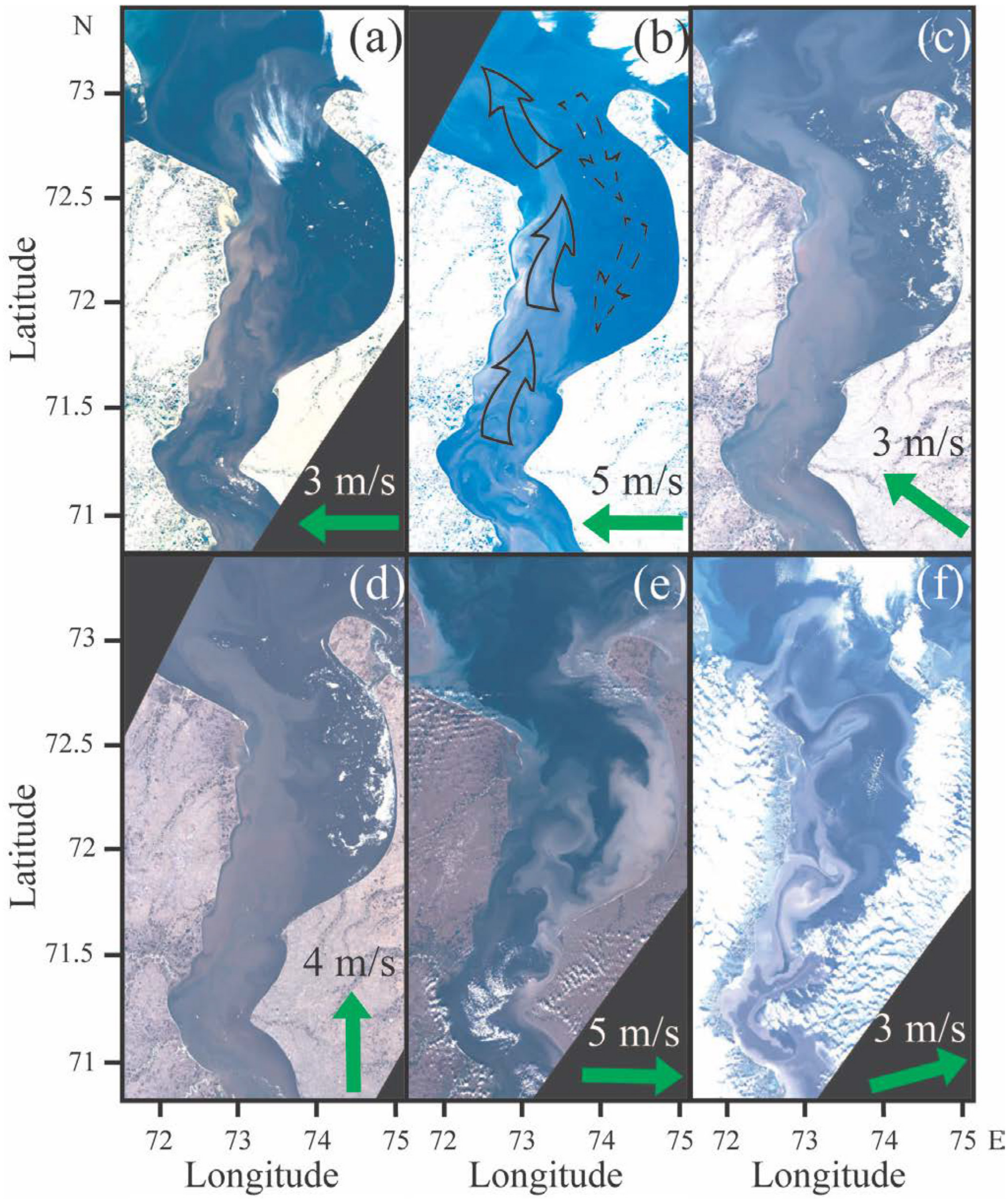

FIGURE 3 | Sentinel-2 optical satellite images of the northern part of the Gulf of Ob acquired on July 4, 2016 **(a)**, July 7, 2016 **(b)**, July 7, 2017 **(c)**, July 16, 2017 **(d)**, September 6, 2018 **(e)**, and August 16, 2020 **(f)**. Green arrows indicate wind forcing during the observation periods. Solid black arrows in panel **(b)** indicate the flow of riverine water from the gulf to the open sea, and dashed black arrows indicate the flow of saline water from the open sea to the gulf.

coefficient is 0.2 (**Figure 6B**). To evaluate the influence of remote wind forcing on saltwater intrusion to the gulf, we calculated the time integrals of downwelling (W_d), upwelling (W_u), offshore (W_{of}), and onshore (W_{on}) wind stress. These wind speed integrals were calculated over the central part of the Kara Sea (73.75–75.5°N, 65.0–85.0°E). The integration is performed over 10 days preceding the middays of the field surveys. Note that the downwelling and offshore wind integrals are positive, and the upwelling and onshore wind integrals are negative. However, to compare all the four wind integrals, we operate with their absolute values, which are shown in **Figure 7**.

Among the four wind integrals, only the upwelling wind shows a good correlation (0.5) with the inflow distance, while the correlations of the downwelling (0.1), onshore (0.2), and offshore (0) winds were low. Large absolute values of the upwelling wind integral (and the respective low values of the downwelling wind

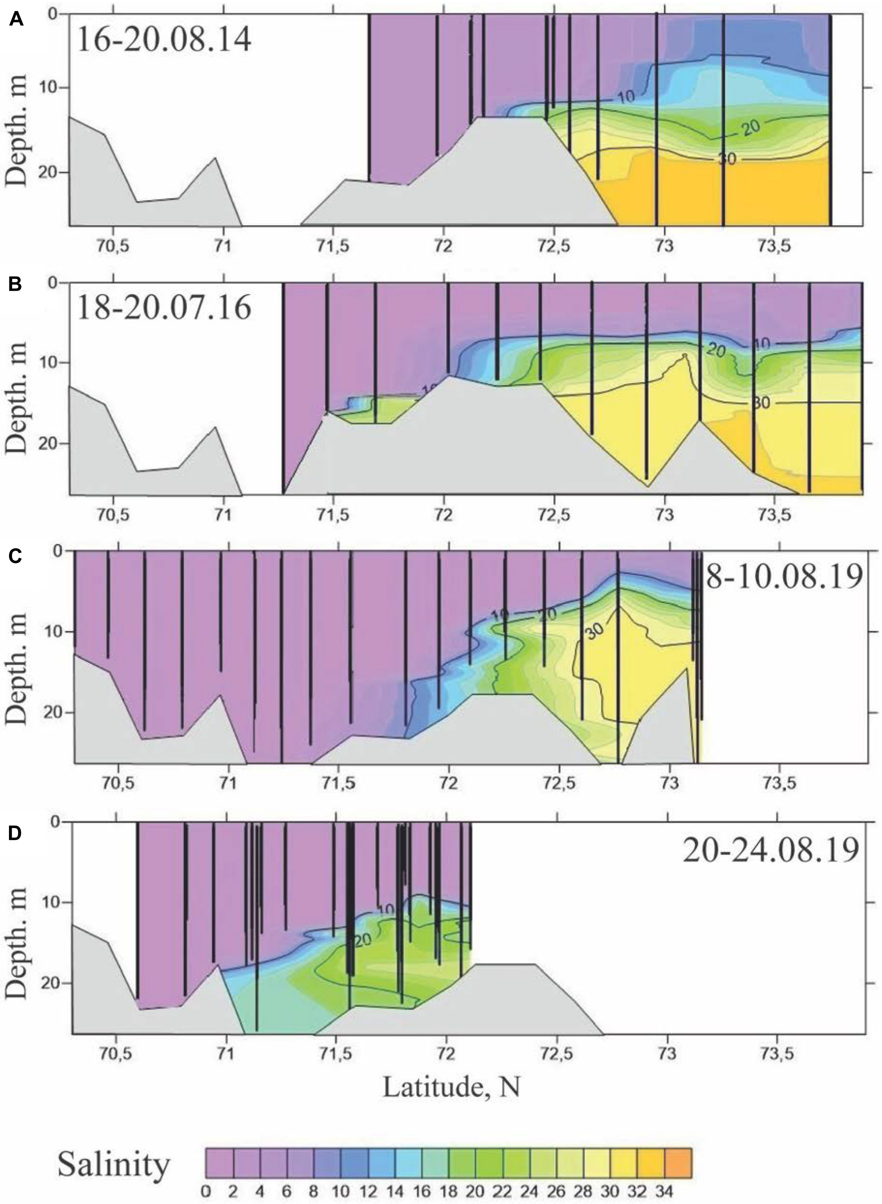

FIGURE 4 | Salinity structure along the transect in the Gulf of Ob on August 16–20, 2014 **(A)**, July 18–20, 2016 **(B)**, August 8–10, 2019 **(C)**, and August 20–24, 2019 **(D)**. Black vertical lines represent salinity measurements at the hydrographic stations.

integral) explain two of the three distant inflows, namely, in July 2016 and August 2019, which were preceded by strong eastern winds. On the other hand, the other wind forcing conditions (except September 2013) were not accompanied by distant inflows, saline waters in these cases propagated only till the latitudes of 72.0–72.3°N. The third registered distant inflow, which occurred in September 2013 (71.6°N), was not preceded by upwelling winds (**Figure 7**). However, it occurred during the drought period in September, and the discharge of the Ob River in 2013 was very low as compared to the other years (**Figure 5**). In particular, the total runoff during the summer freshet in 2013 (270 km^3 or 17,000 m^3/s) was by ~20% lower than the average value in 2007–2019 (325 km^3 or 20,500 m^3/s). Therefore, we associate this moderate inflow with low discharge conditions, i.e., low gravitational forcing, as described by Lapin (2011).

Upwelling Events in the Central Part of the Kara Sea

Strong eastern winds in July 2016 and August 2019 induced upwelling circulation in the central part of the Kara Sea, including the area adjacent to the Gulf of Ob. This process is manifested by the formation of positive sea level anomaly in the central part of the Kara Sea northward from the Gulf

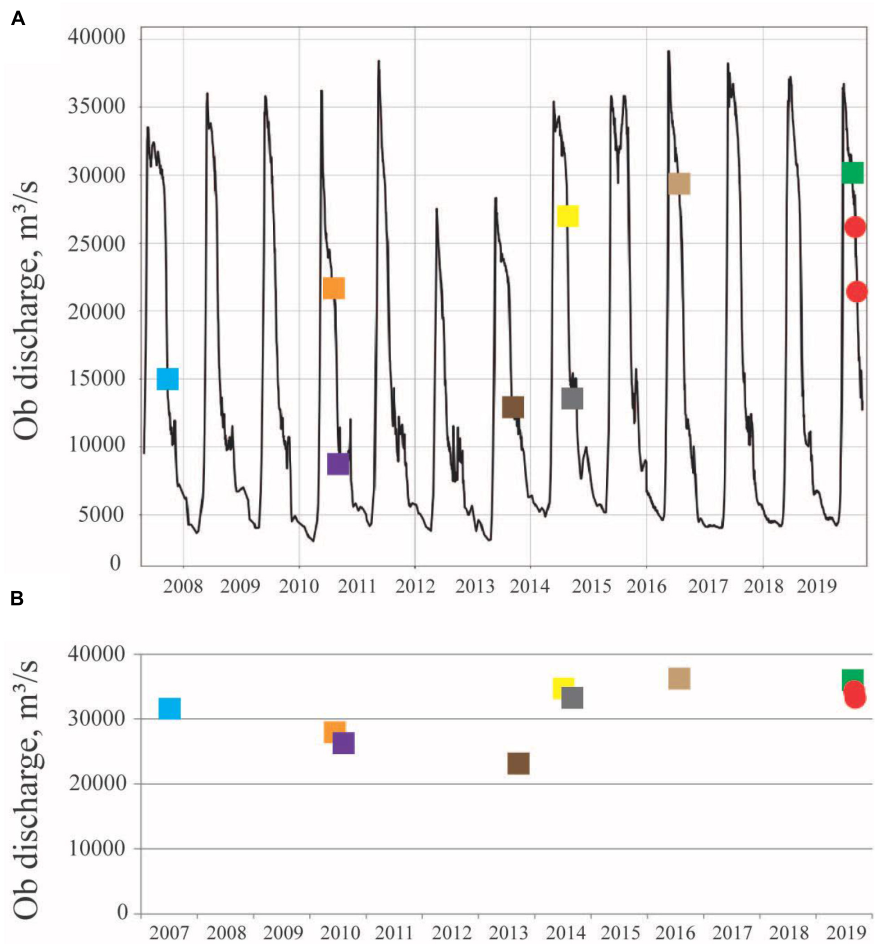

FIGURE 5 | Discharge of the Ob River to the Gulf of Ob in 2007–2019 **(A)** and average discharge from the beginning of summer freshet till the periods of oceanographic field surveys **(B)**. Colored squares and circles in panel **(A)** indicate periods of the oceanographic field surveys as shown in **Figure 2**. Note that the two surveys in August 2019 are indicated by two red circles.

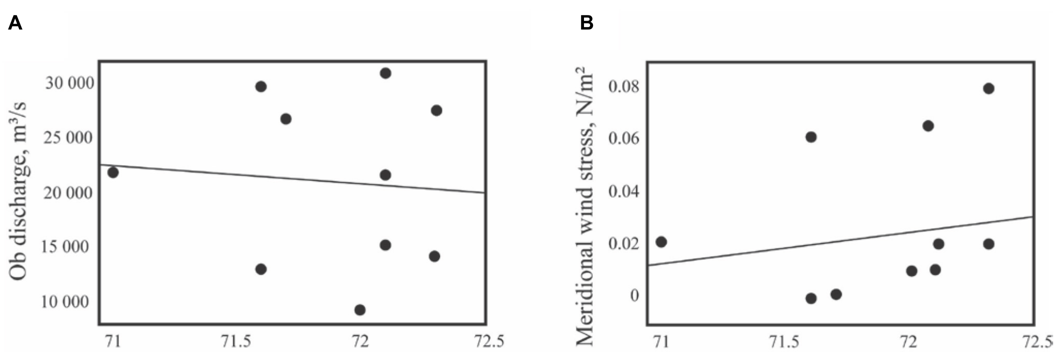

FIGURE 6 | Relations between the discharge rates of the Ob River **(A)** and the along-estuarine wind stress **(B)** with registered distances of saline inflows to the Gulf of Ob during the considered field surveys. Black lines represent the linear trends.

of Ob, which is visible at satellite altimetry data (**Figure 8**). Offshore (northward) flow in the surface layer within the Ob–Yenisei plume and onshore (southward) flow in the bottom layer increased the estuary—sea pressure gradient, which resulted in intensified saltwater intrusion to the gulf. This mechanism of impact of upwelling/downwelling wind events over the open sea

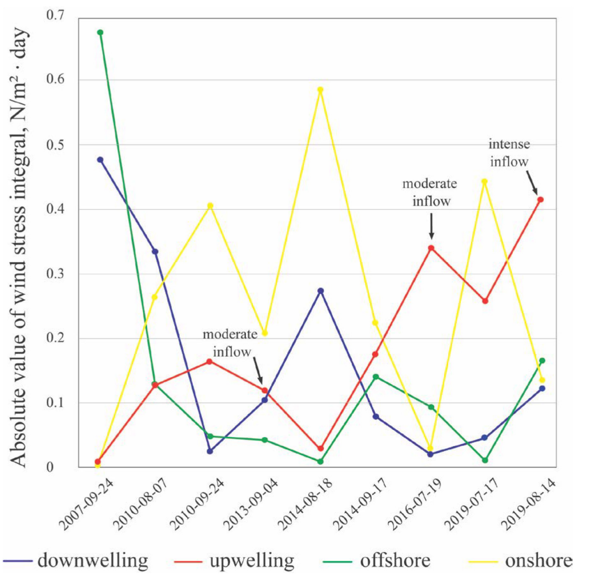

FIGURE 7 | The absolute values of time integrals of downwelling (blue), upwelling (red), offshore (green), and onshore (yellow) wind stress at the central part of the Kara Sea preceding the periods of *in situ* measurements. Black arrows indicate cases with moderate and intense inflows.

on estuarine—sea water exchange was reported earlier for many regions in the World Ocean (Stigebrandt, 1990; Aure et al., 1996; Monteiro and Largier, 1999; Hickey et al., 2002; Hickey and Banas, 2003; Gilcoto et al., 2007) and was explicitly described and analyzed by Giddings and MacCready (2017).

Generally, upwelling events strengthen the barotropic gradient, which increase the horizontal density gradient and the estuarine circulation, and strengthen the baroclinic gradient, which induce the upstream transport of increased salinities. The role of the barotropic effect in the increased saltwater intrusion will be more important because salinity in the bottom layer in front of the Gulf of Ob does not change significantly. The observed variability of salinity is 30–33, which corresponds to variability of density 1,024–1,027 kg/m^3, i.e., ~0.3% of relative variation. The role of the barotropic pressure gradient typically dominates the role of the baroclinic pressure gradient in water exchange processes in large estuaries (Osadchiev, 2017; Zavialov et al., 2020).

Coastal upwelling events are often manifested at optical and thermal satellite imagery by areas of cold (and sometimes turbid) water along the shore once the bottom layer penetrates up to the sea surface near the coast (Osadchiev et al., 2020c). However, during the upwelling events in the Kara Sea, the cold and saline bottom layer does not reach the surface layer near the Gulf of Ob because it is blocked by the Ob plume in this area. Nevertheless, the bottom layer reaches the surface layer eastward from the Gulf of Ob along the coast of Taymyr Peninsula. Therefore, the formation of a turbid and cold stripe in this area visible at satellite imagery (indicated by white arrows in **Figure 9**) is an indicator of general upwelling circulation in the central part of the Kara Sea. Note that no cloud-free satellite imagery is available for the beginning of August 2019; therefore, in **Figure 9** we showed satellite imagery on July 2019, which are the closest dates to the period of field survey with cloud-free images.

In this study, we selected the integration period for the wind speed equal to 10 days because the best correlation between the wind and inflow conditions was provided. This period is a reasonable time lag between atmospheric forcing in the central part of the Kara Sea and the response of the estuarine circulation in the Gulf of Ob. In particular, the period of response of surface layer circulation to wind forcing in the central part of the Kara Sea is equal to several days (Osadchiev et al., 2017), similar temporal periods are registered in the Laptev and East-Siberian seas (Osadchiev et al., 2020c). The onset of the inflow of saline seawater to the gulf located 200–300 km southward from the central part of the Kara Sea requires approximately a week of additional time. The response period of estuarine inflow to remote upwelling winds reported in Giddings and MacCready (2017) is equal to 8 days, which is also consistent with our averaging period equal to 10 days.

In situ measurements performed in the study area confirm that an intense inflow to the gulf in the middle of August 2019 was induced by upwelling winds and was formed during a relatively short time period (**Figures 4C,D**). Variable wind conditions observed in the study area in the first half of July 2019 were accompanied by typical low-inflow conditions (72.1°N) registered on July 16–18, 2019. Then, strong eastern and northeastern winds dominated in the central part of the Kara Sea from July 30, 2019 to August 8, 2019 (**Figure 8B**). It induced an intense inflow of saline seawater to the gulf till the latitude of 71.7°N registered on August 8–10. After August 8 upwelling winds ceased; however, the inertial flow of saline water in the bottom layer in the Gulf of Ob reached the latitude of 71.0°N, which was registered on August 18–20. In July 2016, upwelling winds dominated the regional atmospheric circulation for 8 days in a row and ceased 4 days before the *in situ* measurements. Thus, in both cases distant inflows of saline water to the Gulf of Ob were formed during 8–10 days by the prevailing upwelling winds in the central part of the Kara Sea. However, the upwelling wind forcing was stronger in the first half of August 2019 ($|W_u|$ = 0.4–0.6 N/m^2 × day) than in July 2016 (0.3–0.5 N/m^2 × day), as a result, the inflow was more intense in August 2019 (71.0°N) than in July 2016 (71.6°N).

DISCUSSION

Frequency and Duration of Upwelling Events

The analysis of *in situ* data and wind forcing conditions shows that the moderate/strong upwelling winds in the central part of the Kara Sea induce the moderate/intense inflows of saline seawater to the Gulf of Ob. To estimate the frequency and duration of these inflows, we calculated the absolute value of upwelling wind stress integral $|W_u|$ for every day for the ice-free seasons (July to October) in 1979–2020 using the ERA5 wind reanalysis. Based on the conditions $0.4 > |W_u| > 0.3$ N/m^2 × day for moderate inflows and $|W_u| > 0.4$ N/m^2 × day for intense

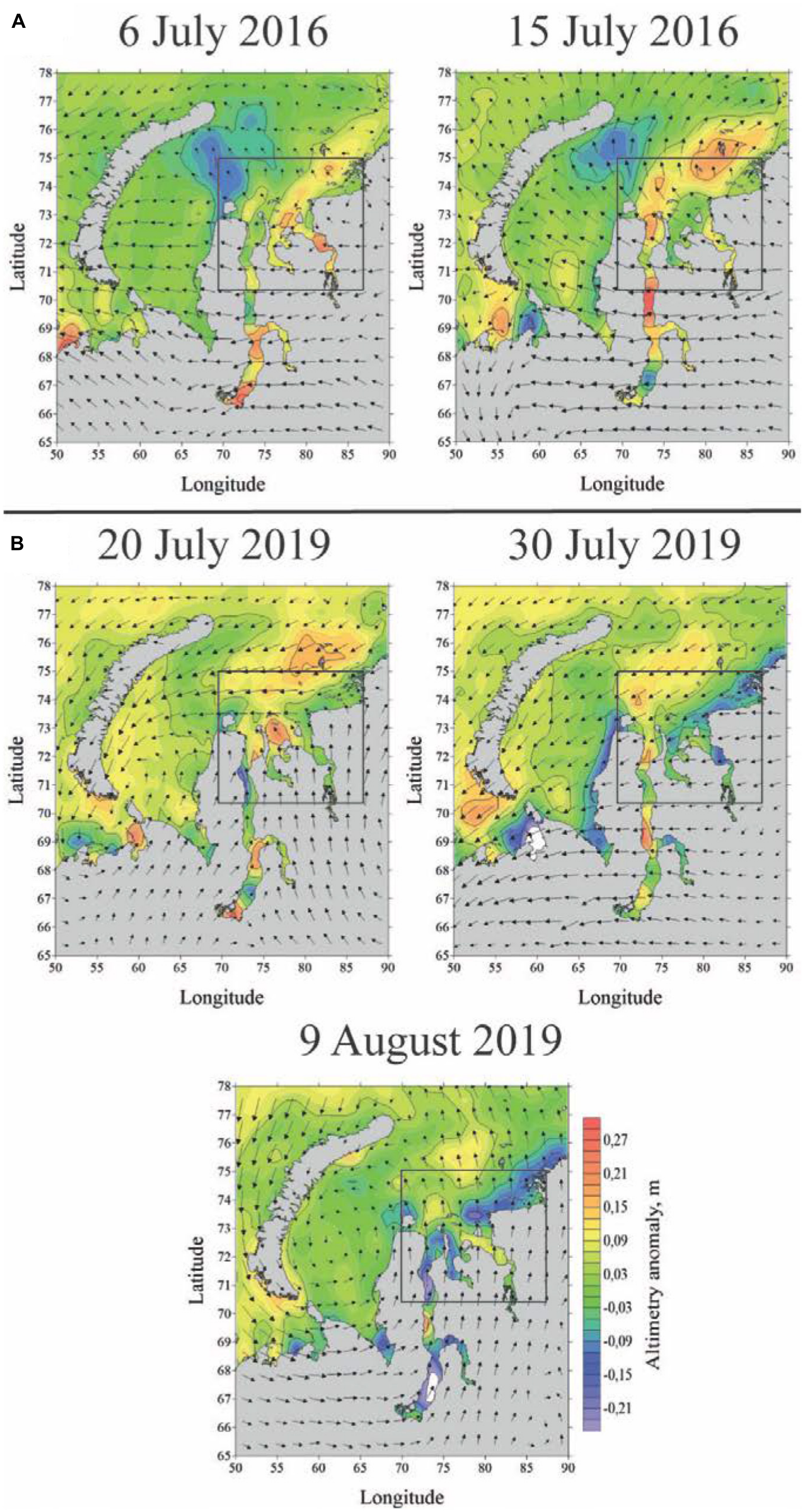

FIGURE 8 | AVISO satellite altimetry anomaly in the Kara Sea on July 6 and July 15, 2016 **(A)**, on July 20, July 30, and August 9, 2019 **(B)**. Black arrows indicate wind direction. Black rectangles indicate the location of area as shown in **Figure 9**.

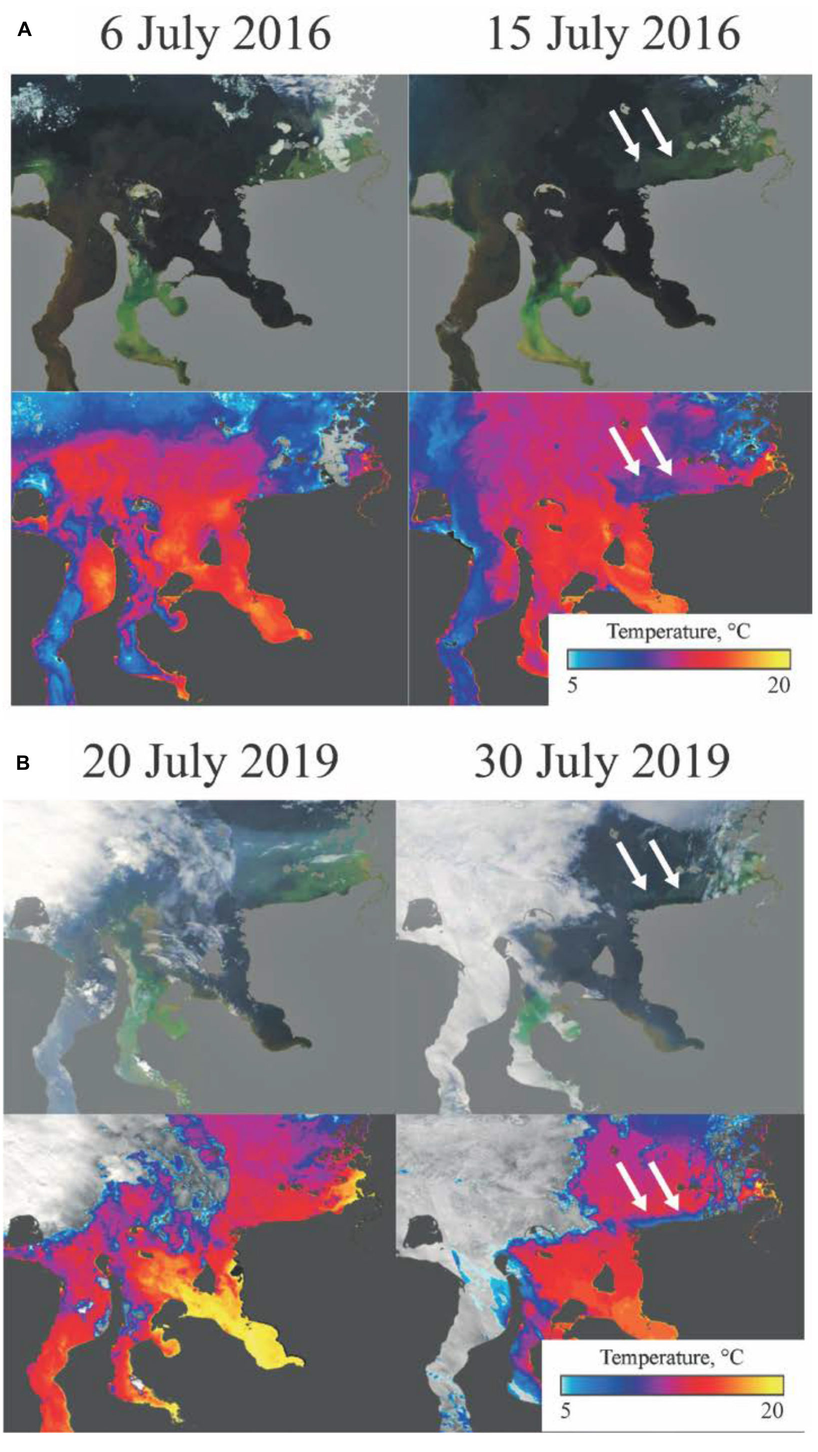

FIGURE 9 | MODIS optical imagery (top panels) and sea surface temperature (bottom panels) in the central part of the Kara Sea on July 6 and July 15, 2016 **(A)**, on July 20 and July 30, 2019 **(B)**. White arrows indicate the location of cold (at thermal images) and turbid (at optical images) surface water along the coast, which manifest upwelling along the Taymyr Peninsula.

inflows, we assessed the periods of wind forcing favorable for the formation of distant inflows to the gulf (**Figure 10**).

Both moderate and intense inflows occurred on average during 26% of days from July to October steadily increasing from 17% in July to 24 and 28% in August and September and then to 35% in October. This feature is caused by intensification of atmospheric circulation in the study region in autumn as compared to summer conditions. The intense inflows have

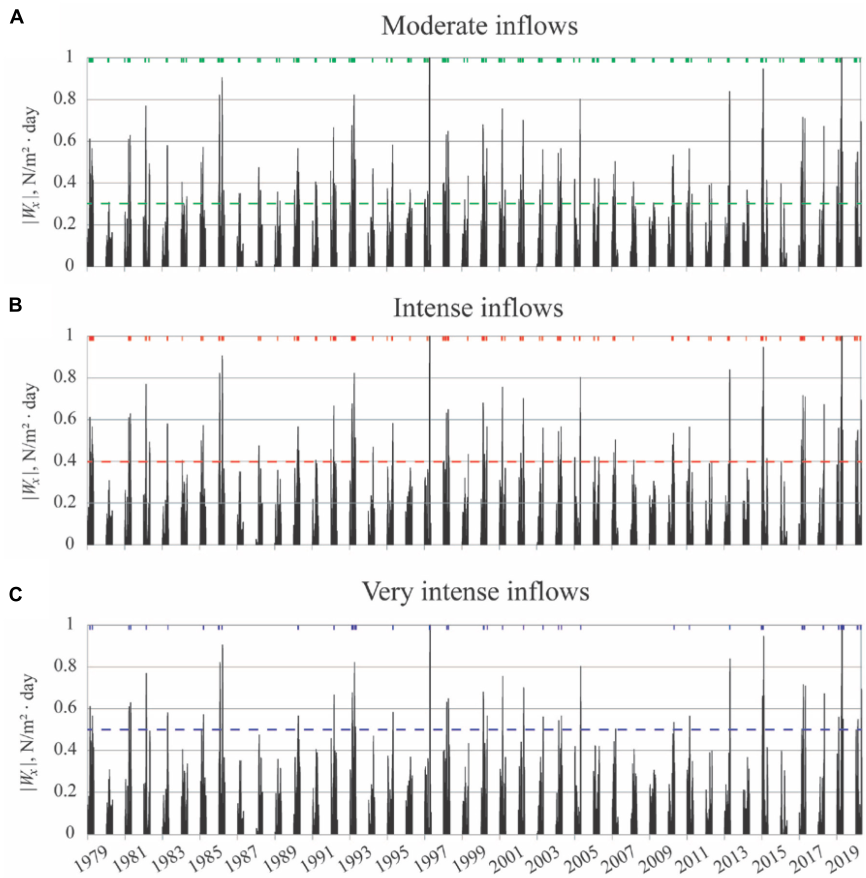

FIGURE 10 | Absolute value of upwelling wind stress integral in the central part of the Kara Sea calculated from the ERA5 atmospheric reanalysis, indicating periods of upwelling-induced moderate inflows (green bars) **(A)**, intense inflows (red bars) **(B)**, and very intense inflows (blue bars) **(C)** to the Gulf of Ob during ice-free seasons (July to October) in 1979–2020. Note that these estimations are based on wind data and not based on *in situ* measurements.

almost the same frequency (14% from July to October, 6% in July, 14% in August, 14% in September, and 22% in October) as the moderate inflows (12% from July to October, 11% in July, 10% in August, 14% in September, and 13% in October). Extremely intense inflows ($|W_u| > 0.5$ N/m^2 $\times$ day), which were not yet detected by *in situ* measurements, occur relatively rarely (5% from July to October, 1% in July, 6% in August, 5% in September, and 9% in October), but they can result in even more distant salt intrusion to the gulf than the observed extent to 71.0°N. The duration of the distant inflows varied from several days to 1 month. The total annual duration of periods of distant inflows varied from 67 days in 1979 and 64 days in 1993 to 5 days in 1999 and 9 days in 2009 due to significant inter-annual variability of local atmospheric circulation (**Figure 11**).

Phytoplankton Communities in the Gulf of Ob

Phytoplankton populations in the Gulf of Ob were addressed in a number of studies during the previous years. Phytoplankton productivity strongly depends on hydrological regime in the gulf and, therefore, has distinct seasonal variability. The spring bloom, which is formed mainly by diatoms shortly after ice melting, shifts to a steady decrease of abundance and biomass till the ice formation period (Makarevich, 2008). Generally, three zones with different phytoplankton communities are distinguished, namely, the freshwater zone with maximal productivity, the frontal zone with a distinct two-layered structure and bottom salinities increasing from 5–6 to 18–20 characterized by an abrupt decrease of productivity, and the saline zone with highly variable phytoplankton characteristics (Druzhkov and Makarevich, 1996; Makarevich et al., 2003; Sukhanova et al., 2010, 2018). However, the field surveys, which are reported in these papers, were performed during different seasons and were limited to certain zones within the gulf, i.e., not covering all the three zones within one survey. As a result, the dependence of phytoplankton communities on highly variable salinity conditions in the gulf still remains unaddressed.

The intensity of propagation of saline seawater to the Gulf of Ob affects local phytoplankton communities and, therefore, modifies the biological productivity in the gulf. In this study, we compare the characteristics of phytoplankton communities observed during the same successional season in the central and northern part of the Gulf of Ob in September 2007,

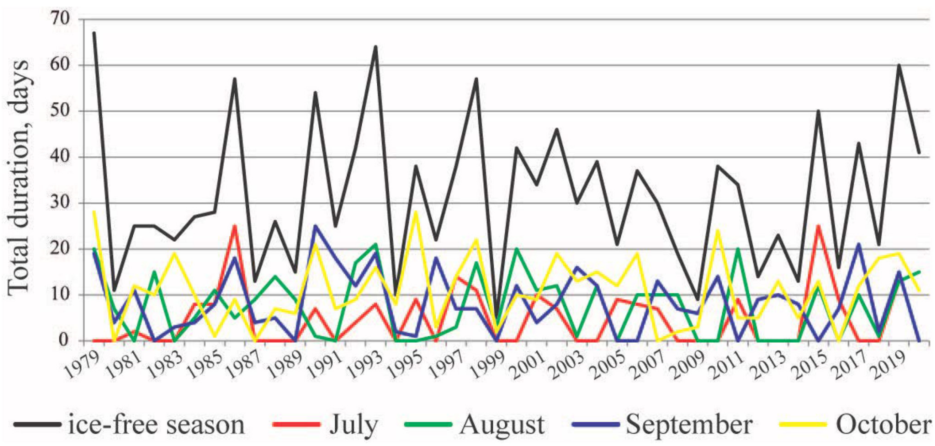

FIGURE 11 | Total annual durations of upwelling-induced distant inflow periods calculated from the ERA5 atmospheric reanalysis during July (red line), August (green line), September (blue line), October (yellow line), and during the whole ice-free season (black line) in 1979–2020. Note that these estimations are based on wind data and not based on *in situ* measurements.

September 2014, and August 2019 during different seawater inflow conditions. In the first and second case, the inflow of saline seawater to the gulf was small, while the third case was accompanied by the development of an intense inflow. As a result, the distribution of phytoplankton in both 2007 and 2014 was significantly different from that in 2019.

Figure 12 illustrates the biomass of phytoplankton and number of cells at the stations along the transects in the gulf. In 2007 and 2014, the maximal biomass and the maximal number of cells were registered in the fresh zone of the gulf (in 2014 also the second maximum of biomass was registered ∼15 km northward from the fresh zone), while further northward the productivity of phytoplankton communities steadily decreases. In particular, in September 2007, the biomass of phytoplankton decreased by 10 times (from 207 to 21 mg/m^3) with an increase of bottom salinity from 0 to 12. In August 2019, on the opposite, the maximal biomass of phytoplankton (1,200 mg/m^3) was observed not in the fresh zone, but at bottom salinities of 10–18. Southward from this area, phytoplankton biomass steadily decreased to 400–600 mg/m^3 in the fresh zone. The number of cells in August 2019 also decreased from 1,000–1,500 million at the latitudes of 71.6–72.2°N to 200–400 in the fresh zone at the latitudes of 70.8–71.4°N.

The qualitative characteristics of phytoplankton communities at different zones within the Gulf of Ob during the considered periods are illustrated by their taxonomical structure certain stations (**Figure 13**). We show the distribution of taxa *Bacillariophyta*, *Dinophyta*, and *Chlorophyta*, while Flagellatae determines a group of flagellated unicellular organisms comprising *Cryptophyta* and *Euglenophyta*. The other taxa in **Figure 13** determine mainly *Cyanobacteria* and other minor taxa. The typical distribution of phytoplankton taxa in the study area described in previous studies was observed in September 2007 and September 2014. Freshwater diatoms, green algae, and cyanobacteria dominate in the fresh zone with the presence of *Euglenophyta* and a small amount of freshwater dinoflagellates. The genus *Aulacoseira* is the most abundant among the freshwater diatoms in the Gulf of Ob. It has a proportional number of cells and biomass and is registered in all seasons. The amount of green algae is decreased in the frontal zone, euglenids steadily disappear, and the amount of dinophytes steadily increases toward the open sea, while the diatoms dominate. At the same time, algae of the genus *Aulacoseira*, which are able to live in brackish water, still dominate in the phytoplankton community of the frontal zone together with other brackish and marine species of the genera *Thalassionema*, *Thalassiosira*, etc. The marine zone of the gulf is characterized by an increase in the amount of dinophytes, which dominate together with diatoms (genera *Thalassionema*, *Thalassiosira*, *Chaetoceros*, etc.). Phylum *Cryptophyta* also contributes to the phytoplankton community in the marine zone, while *Chlorophyta*, *Euglenophyta*, and *Cyanobacteria* are almost completely absent. The largest difference in the taxonomical structure of the phytoplankton communities between September 2007 and September 2014 consists of a significantly lower amount of large diatom algae in the later stage, which results in different ratios of number of cells and biomass (**Figure 13**).

The distribution of phytoplankton communities in the Gulf of Ob in August 2019 was significantly different from those observed in September 2007 and September 2014. Dominance of diatom algae was maximal in August 2019. Diatoms provided 80–98% of total biomass at the majority of stations with bottom salinities equal to 20–25, which were located at the latitudes of 71.6–72.4°N. This large share was associated with an increase in the amount of brackish water species of the genera *Thalassionema*, *Thalassiosira*, *Melosira*, etc. The share of species of *Aulacoseira* was 52–76%, while in 2007 this share at the same salinities was equal to 24–34%.

In accordance with the abovementioned successional cycle, the spring bloom after ice melting occurs due to the development of diatoms, as was observed at the end of July 2016 (Sukhanova et al., 2018). Blooming occurs due to diatoms of all ecological

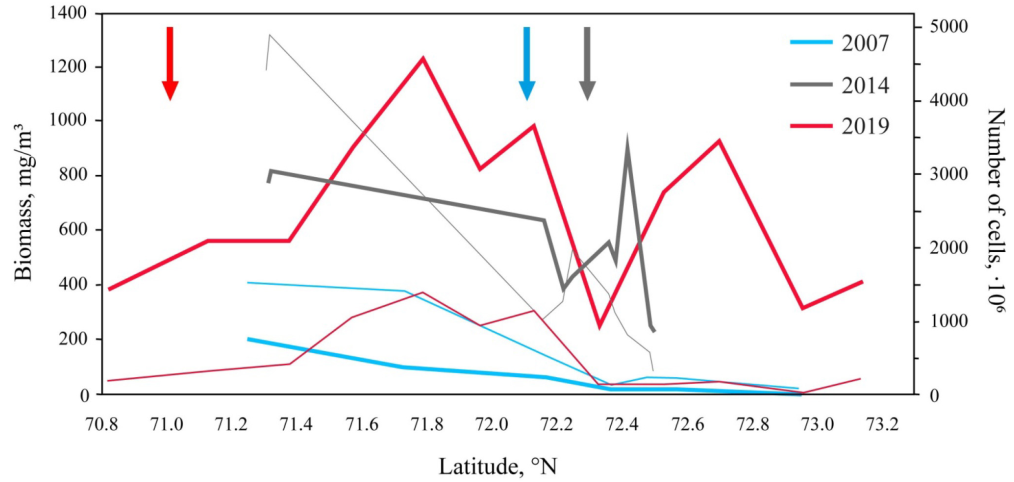

FIGURE 12 | Phytoplankton biomass (thick lines) and the number of cells (thin lines) in 2007 (blue), 2014 (gray), and 2019 (red). Arrows indicate southernmost detected locations of the isohaline of five in the bottom layer in the Gulf of Ob.

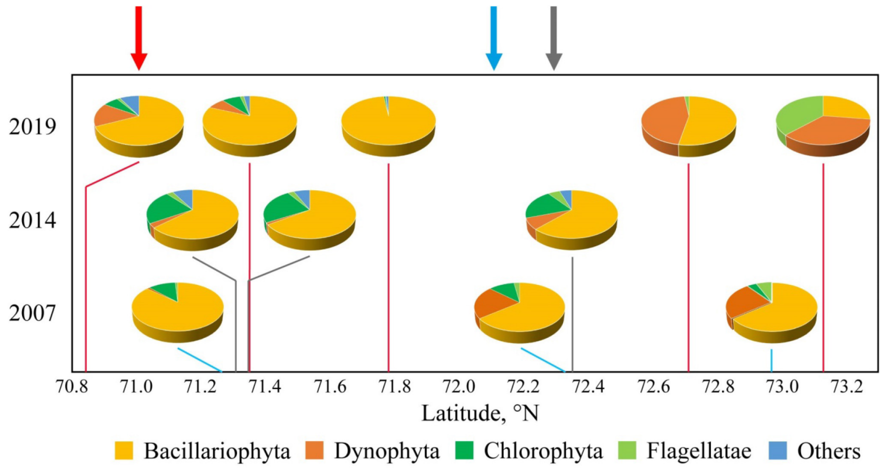

FIGURE 13 | Taxonomical structure of phytoplankton communities in 2007 (blue), 2014 (gray), and 2019 (red) at different zones within the Gulf of Ob. Arrows indicate southernmost detected locations of the isohaline of five in the bottom layer of the Gulf of Ob.

groups, namely, freshwater, marine, and brackish. It is followed by a decline in quantitative indicators and an increase of species ratio of freshwater algae due to *Cyanophyta* and *Chlorophyta* in the frontal zone, as was observed in September 2007 and September 2014. In September 2019, on the opposite, the number of diatoms remained high throughout seasonal, salinity and longitudinal distribution in the gulf, the same was observed for common indices of abundance and biomass. At the same time, the taxonomic diversity of the extended frontal zone decreases in contrast to euryhaline or brackish water diatom species (Olli et al., 2019). This feature can be caused by two factors. First, the distant advection of saline seawater results in the development of brackish water algae at a large area in the Gulf of Ob. Second, upwelling-advected seawater is especially rich in nutrients because active reproduction of diatoms at this season can occur only in the presence of high silicon content in seawater, which is non-typical for this area (Ardyna and Arrigo, 2020). The freshwater species are almost absent at the saline zone of the gulf in August 2019, which is typical for the open part of the Kara Sea. *Dinophyta* and *Cryptophyta* phylums together with marine diatom species dominated in this zone in August 2019. In September 2007 and September 2014, however, freshwater species of green and euglena algae were present in the surface layer of the saline zone.

CONCLUSION

In this study, we address the water exchange between the Gulf of Ob and the open part of the Kara Sea during ice-free periods. Based on the analysis of the extensive *in situ* measurements performed in 2007–2019, we reconstruct a dependency between the distance of saline water inflow to the gulf and external forcing conditions. We show that the large freshwater runoff during the warm season causes the domination of gravitational circulation in the gulf and the formation of a strong two-layered stratification in the northern part of the gulf. Under average climatic conditions, saline seawater occupies the bottom layer only till the latitudes of 72.0–72.3°N. Further southward, the gulf water have zero salinity from surface to bottom. Seasonal and inter-annual variability of the freshwater runoff results in northern-southern shifts of this boundary between saline and fresh water in the bottom layer, albeit not exceeding 50–70 km. In particular, in 2013, which is characterized by the lowest annual discharge conditions among the analyzed years and the second lowest freshet runoff in the last 25 years, this boundary was located at the latitude of 71.6°N. In the presence of large longitudinal density gradient and vertical stratification, tidal circulation and local wind forcing limitedly affect the general structure of estuarine circulation. Strong wind forcing over the Gulf of Ob can modify estuarine circulation and mixing in case of strong northern or southern winds ($\sim$10 m/s), albeit these conditions occur in only 4% of days during the ice-free season.

The estuarine processes in the Gulf of Ob experience a much stronger influence from remote wind forcing, namely, upwelling winds over the central part of the Kara Sea can cause intense and distant inflows of saline seawater to the Gulf of Ob. In this case, the offshore flow in the surface layer in the area adjacent to the Gulf of Ob and the onshore flow in the bottom layer increase the estuarine—sea barotropic pressure gradient, which results in the intensified transport of seawater to the gulf. Under these conditions, the observed distance of salt intrusion to the gulf is 120–170 km and depends on the intensity and duration of the related upwelling event. This process has synoptic variability, i.e., the response period of an estuarine inflow to remote upwelling wind is equal to 1–2 weeks. Particularly, in August 2019, the southern border of saline seawater in the gulf moved from 71.7°N to 71.0°N, i.e., it was shifted by $\sim$80 km in less than 10 days. The upwelling-induced inflow of saline seawater is a typical process in the Gulf of Ob, these inflows occur for a quarter of days during the ice-free season. The frequency of these inflows increases from 17% in July to 35% in October, which indicates that the estuarine—sea water exchange significantly intensifies in autumn.

The results obtained for the water exchange between the Gulf of Ob and the Kara Sea can be applied for other coastal areas where large estuarine rivers inflow to sea. Once a large river discharge dominates estuarine circulation and stratification, local wind straining and surface mixing are not strong enough to affect estuarine processes. However, the same wind speed can affect circulation in the adjacent ocean, which is less stratified and has smaller pressure gradient. Thus, remote upwelling can be the only wind-induced process that can influence circulation in stable estuaries, which receive a large amount of freshwater discharge. Also, we want to highlight the fundamental difference between the response of circulation at stratified inner-shelf on upwelling- and downwelling-favorable wind forcing (Lentz and Fewings, 2012). The wind-induced upwelling circulation results in the formation of a constant inflow of high-saline water toward the shore, which maintains the inner-shelf stratification. Once this process occurs in front of a large estuary, it stably enhances the estuarine—sea water exchange. The wind-induced downwelling circulation, on the opposite, causes the onshore flow of freshened water, which tends to inhibit stratification and to weaken the cross-shelf circulation at the inner-shelf. However, freshwater discharge from a large estuary supports stratification. As a result, downwelling circulation occurs seaward from the estuary and limitedly affects the estuarine—sea water exchange.

The upwelling-induced distant salt intrusions strongly modify biological productivity in the Gulf of Ob. First, the distant intrusions of nutrient-rich seawater refresh the content of nutrients in the gulf. Once nutrients are naturally released in the biogeochemical cycle, algae rapidly multiply that results in an additional bloom, which is similar to the spring situation. On the other hand, the upwelling-induced distant salt intrusions significantly enhance the phytoplankton productivity within the gulf by an increase of biomass of just several species of brackish water or euryhaline species of diatoms. Therefore, long-term and frequent upwelling events during certain months and years would cause a shift in taxonomical structure or decrease of species richness in phytoplankton community together with an increase of its quantitative features. As a result, the distribution of species will shift to a similar group of zooplankton, which has adaptation for life in the brackish water conditions (Drits et al., 2017). Finally, frequent upwelling events can strongly modify seasonal variability of plankton communities and food webs within the Gulf of Ob, which is typical for estuaries (Moller et al., 2009). Species richness is an important indicator for the assessment of the anthropogenic influence on the Gulf of Ob; therefore, the effect of an upwelling-induced shift should be considered while estimating the cumulative impact of industrial development in the gulf on the local ecosystem.

The circulation and mixing regimes in the Gulf of Ob are fundamentally different during winter-spring and summer-autumn seasons due to two main factors. First, very large seasonal variability of freshwater discharge (>10 times between cold and warm seasons) provides a dramatic increase of the longitudinal density gradient and the vertical stratification in the gulf during the warm season. Second, the ice coverage in the cold season isolates water in the gulf (as well as in the Kara Sea) from atmospheric forcing and increases mixing of the surface layer as compared to the warm season. As a result, during winter time circulation and vertical stratification in the gulf relax, while salinity increases. However, in this study, we focused on the estuarine processes in the Gulf of Ob only during the warm season. The related processes during the cold season remain almost unaddressed due to the lack of *in situ* measurements and require a specific study.

The distant inflows of saline seawater can strongly affect the delivery and fate of suspended sediments in the Gulf of Ob. The average concentration of total suspended matter in the Ob runoff is $\sim$0.4 g/m^3, which results in the annual sediment discharge of 16.5 $\times$ 10^6 tons (Gordeev et al., 1996). Mixing of river runoff and saline seawater causes the intense sedimentation deposit in the northern part of the gulf (43–1,120 g/m^2 day), in particular, the sediment accumulation velocity within the ship channel is up to 0.2–0.35 m/year (Logvina et al., 2012; Gladysh et al., 2017;

Vvedensky et al., 2017). As a result, frequent and intense inflows of saline seawater to this area can induce the resuspension of bottom sediments and significantly modify local transport and deposition pathways, which was reported for many river estuaries (Festa and Hansen, 1978; Burchard and Baumert, 1998; Li et al., 2011; Burchard et al., 2018) and the adjacent coastal regions (Osadchiev et al., 2016; Osadchiev and Korshenko, 2017).

The results of this study also have certain implications for the ongoing engineering activities in the Gulf of Ob caused by an increase of regional maritime shipping in the last decade. The ship channel (50 km long, 500–600 m wide, and 15 m deep) was constructed in 2015 and connects the central (71.9°N) and northern (72.6°N) part of the gulf. Several previous studies used numerical modeling to assess the influence of this channel on salt intrusion to the central part of the gulf (Dianskiy et al., 2015; Vvedensky et al., 2017). Our results demonstrate that the distance of seawater inflow through the ship channel as a gravity current under average conditions as well as the volume of salt intrusion are negligible as compared to those provided by regular upwelling-induced inflows described in this study.

Finally, the process of mixing of saline seawater and river discharge in the Gulf of Ob determines the initial formation of the Ob–Yenisei plume, which spreads over a wide area in the Kara Sea and is among the largest freshwater reservoirs in the Arctic Ocean. As a result, the study on the formation of the Ob–Yenisei plume is important for understanding many local processes in the Kara Sea, including circulation (Osadchiev et al., 2017, 2020a, 2021a), sediment transport (Osadchiev et al., 2019), carbon cycle and acidification (Polukhin, 2019), anthropogenic pollution (Pogojeva et al., 2021; Yakushev et al., 2021), as well as the large-scale freshwater transport in the Eastern Arctic (Haine et al., 2015; Janout et al., 2015; Carmack et al., 2016; Nummelin et al., 2016; Osadchiev et al., 2020b, 2021b).

DATA AVAILABILITY STATEMENT

The ERA5 reanalysis data were downloaded from the European Centre for Medium-Range Weather Forecasts (ECMWF) website https://www.ecmwf.int/en/forecasts/datasets/reanalysis-datasets/era5. The river discharge data were downloaded from the Arctic Great Rivers Observatory (ArcticGRO) website https://arcticgreatrivers.org/data/. The wind data from the Seyakha meteorological station were downloaded from https://rp5.ru/. The Sentinel-2 L2 products were downloaded from the Copernicus Open Access Hub (https://scihub.copernicus.eu/). The MODIS L1b products were downloaded from the NASA web repository (https://ladsweb.modaps.eosdis.nasa.gov/). The AVISO altimetry products were downloaded from the AVISO web repository (https://www.aviso.altimetry.fr/).

AUTHOR CONTRIBUTIONS

AO designed the study. AO and OK organized the database and wrote the first draft of the manuscript. AO, OK, and AG performed the analysis of the *in situ* and meteorological data. All authors contributed to manuscript revision, read, and approved the submitted version.

FUNDING

This research was funded by the Ministry of Science and Higher Education of the Russian Federation, theme 0128-2021-0001 (collecting of in situ data), the Grant of the President of the Russian Federation for state support of young Russian scientists-candidates of science, research project MK-98.2020.5 (processing of in situ data), and the Russian Foundation for Basic Research 20-35-70039 (study of FSL).

ACKNOWLEDGMENTS

The authors would like to thank Yamal LNG company for support of field survey in the Gulf of Ob in August 2019.

REFERENCES

Ardyna, M., and Arrigo, K. R. (2020). Phytoplankton dynamics in a changing Arctic Ocean. *Nat. Clim. Chang.* 10, 892–903. doi: 10.1038/s41558-020-0905-y

Aure, J., Molvær, J., and Stigebrandt, A. (1996). Observations of inshore water exchange forced by a fluctuating offshore density field. *Mar. Poll. Bull.* 33, 112–119. doi: 10.1016/S0025-326X(97)00005-2

Borisenko, G. V., Makkaveev, E. P., and Stunzhas, P. A. (2021). Concentration and diffusion of nutrients in the interpore–bottom water system of the Ob River estuary. *Oceanology* 61, 25–33. doi: 10.1134/S0001437020060028

Burchard, H., and Baumert, H. (1998). The formation of estuarine turbidity maxima due to density effects in the salt wedge. A hydrodynamic process study. *J. Phys. Oceanogr.* 28, 309–321.

Burchard, H., Schuttelaars, H. M., and Ralston, D. K. (2018). Sediment trapping in estuaries. *Annu. Rev. Mar. Sci.* 10, 371–395. doi: 10.1146/annurev-marine-010816-060535

Carmack, E. C., Yamamoto–Kawai, M., Haine, T. W., Bacon, S., Bluhm, B. A., Lique, C., et al. (2016). Freshwater and its role in the Arctic Marine System: Sources, disposition, storage, export, and physical and biogeochemical consequences in the Arctic and global oceans. *J. Geophys. Res. Biogeosci.* 121, 675–717. doi: 10.1002/2015JG003140

Chawla, A., Jay, D. A., Baptista, A. M., Wilkin, M., and Seaton, C. (2008). Seasonal variability and estuary-shelf interactions in circulation dynamics of a river-dominated estuary. *Estuar. Coasts* 31, 269–288. doi: 10.1007/s12237-007-9022-7

Chen, S. N., and Sanford, L. P. (2009). Axial wind effects on stratification and longitudinal salt transport in an idealized, partially mixed estuary. *J. Phys. Oceanogr.* 39, 1905–1920. doi: 10.1175/2009JPO4016.1

Dianskiy, N., Fomin, V., Kabatchenko, I., Litvinenko, G., and Gusev, A. (2015). "Assessing the impact of the planned approach channel to the seaport Sabetta on salinity changes in the Gulf of Ob," in *Proceedings of the 23rd International Conference on Port and Ocean Engineering under Arctic Conditions*, (Trondheim: University of Science and Technology (NTNU)), 1–12.

Drits, A. V., Pasternak, A. F., Nikishina, A. B., Semenova, T. N., Sergeeva, V. M., Polukhin, A. A., et al. (2016). The dominant copepods Senecella siberica and *Limnocalanus macrurus* in the Ob estuary: ecology in a high-gradient environment. *Polar Biol.* 39, 1527–1538. doi: 10.1007/s00300-015-1878-6

Drits, A., Pasternak, A., and Flint, M. (2017). Distribution and grazing of dominant zooplankton species in the Ob estuary: Influence of the runoff regime. *Estuar. Coasts* 40, 1082–1095. doi: 10.1007/s12237-016-0201-2

Druzhkov, N. V., and Makarevich, P. R. (1996). *Spatiotemporal Organization of Phytocenosis in Open Shelf Waters of the Western Arctic, Ecosystems of the Pelagic Zone of the Western Arctic Seas*. Apatity: Kol'sk, 37–72.

Festa, J. F., and Hansen, D. V. (1978). Turbidity maxima in partially mixed estuaries: a two-dimensional numerical model. *Estuar. Coast. Mar. Sci.* 7, 347–359. doi: 10.1016/0302-3524(78)90087-7

Flint, M. V., and Poyarkov, S. G. (2015). Comprehensive research on the Kara Sea ecosystem (128th cruise of Research Vessel Professor Shtokman). *Oceanology* 55, 657–659. doi: 10.1134/S0001437015040074

Flint, M. V., Poyarkov, S. G., Rimsky-Korsakov, N. A., and Miroshnikov, A. Y. (2020). Ecosystems of Siberian Arctic Seas-2019: Spring processes in the Kara Sea (Cruise 76 of the R/V Akademik Mstislav Keldysh). *Oceanology* 60, 134–137. doi: 10.1134/S0001437020010105

Geyer, W. R. (1997). Influence of wind on dynamics and flushing of shallow estuaries. *Estuar. Coast. Shelf Sci.* 44, 713–722. doi: 10.1006/ecss.1996.0140

Geyer, W. R., and MacCready, P. (2014). The estuarine circulation. *Annu. Rev. Fluid Mech.* 46, 175–197. doi: 10.1146/annurev-fluid-010313-141302

Giddings, S. N., and MacCready, P. (2017). Reverse estuarine circulation due to local and remote wind forcing, enhanced by the presence of along-coast estuaries. *J. Geophys. Res. Oceans* 122, 10184–10205. doi: 10.1002/2016JC012479

Gilcoto, M., Pardo, P. C., Alvarez-Salgado, X. A., and Perez, F. F. (2007). Exchange fluxes between the Ria de Vigo and the shelf: A bidirectional flow forced by remote wind. *J. Geophys. Res.* 112:C06001. doi: 10.1029/2005JC003140

Gladysh, V. A., Logvina, E. A., Nesterov, A. V., and Kubishkin, N. V. (2017). Assessing the intensity of lithodynamic processes in the seaway navigation canal of the sabetta port. *Eng. Surv.* 4, 36–45. doi: 10.25296/1997-8650-2017-4-36-44

Gordeev, V. V., Martin, J. M., Sidorov, J. S., and Sidorova, M. V. (1996). A reassessment of the Eurasian river input of water, sediment, major elements, and nutrients to the Arctic Ocean. *Am. J. Sci.* 296, 664–691. doi: 10.2475/ajs.296.6.664

Guay, C. K., Falkner, K. K., Muench, R. D., Mensch, M., Frank, M., and Bayer, R. (2001). Wind-driven transport pathways for Eurasian Arctic river discharge. *J. Geophys. Res.* 106, 11469–11480. doi: 10.1029/2000JC000261

Haine, T. W. N., Curry, B., Gerdesc, R., Hansend, E., Karcherce, M., Lee, C., et al. (2015). Arctic freshwater export: status, mechanisms, and prospects. *Glob. Planet. Change* 125, 13–35. doi: 10.1016/j.gloplacha.2014.11.013

Hansen, D. V., and Rattray, M. (1965). Gravitational circulation in straits and estuaries. *J. Mar. Res.* 23, 104–122.

Harms, I. H., and Karcher, M. J. (1999). Modeling the seasonal variability of circulation and hydrography in the Kara Sea. *J. Geophys. Res.* 104, 13431–13448. doi: 10.1029/1999jc900048

Hersbach, H., Bell, B., Berrisford, P., Hirahara, S., Horányi, A., Muñoz-Sabater, J., et al. (2020). The ERA5 global reanalysis. *Q. J. R. Meteorol. Soc.* 146, 1999–2049. doi: 10.1002/qj.3803

Hickey, B. M., and Banas, N. S. (2003). Oceanography of the US Pacific Northwest coastal ocean and estuaries with application to coastal ecology. *Estuaries* 26, 1010–1031. doi: 10.1007/BF02803360

Hickey, B. M., Zhang, X., and Banas, N. (2002). Coupling between the California current System and a coastal plain estuary in low riverflow conditions. *J. Geophys. Res.* 107:3166. doi: 10.1029/1999JC000160

Hillebrand, H., Dürselen, C.-D., Kirschel, D., Pollinger, U., and Zohary, T. (1999). Biovolume calculation for pelagic and benthic microalgae. *J. Phycol.* 35, 403–424. doi: 10.1046/j.1529-8817.1999.3520403.x

Janout, M. A., Aksenov, Y., Holemann, J. A., Rabe, B., Schauer, U., Polyakov, I. V., et al. (2015). Kara Sea freshwater transport through Vilkitsky Strait: variability, forcing, and further pathways toward the western Arctic Ocean from a model and observations. *J. Geophys. Res. Oceans* 120, 4925–4944. doi: 10.1002/2014JC010635

Kagan, B. A., Timofeev, A. A., and Sofina, E. V. (2010). Seasonal variability of surface and internal M2 tides in the Arctic Ocean. *Izv. Atmos. Ocean. Phys.* 46, 652–662. doi: 10.1134/S0001433810050105

Lange, X., and Burchard, H. (2019). The relative importance of wind straining and gravitational forcing in driving exchange flows in tidally energetic estuaries. *J. Phys. Oceanogr.* 49, 723–736. doi: 10.1175/jpo-d-18-0014.1

Lange, X., Klingbeil, K., and Burchard, H. (2020). Inversions of estuarine circulation are frequent in a weakly tidal estuary with variable wind forcing and seaward salinity fluctuations. *J. Geophys. Res. Oceans.* 125:e2019JC015789. doi: 10.1029/2019JC015789

Lapin, S. A. (2011). Hydrological characterization of the Ob' Inlet in the summer and autumn seasons. *Oceanology* 51, 925–934. doi: 10.1134/S0001437011060105

Lapin, S. A., Artamonova, K. V., Gangnus, I. A., and Kivva, K. K. (2015). Hydrological and chemical characteristics of the frontal zone in the Gulf of Ob in early autumn. *Probl. Arct. Antarct.* 3, 15–26.

Lentz, S. J., and Fewings, M. R. (2012). The wind- and wave-driven inner-shelf circulation. *Annu. Rev. Mar. Sci.* 4, 317–343. doi: 10.1146/annurev-marine-120709-142745

Li, C., White, J. R., Chen, C., Lin, H., Weeks, E., Galvan, K., et al. (2011). Summertime tidal flushing of Barataria Bay: transports of water and suspended sediments. *J. Geophys. Res. Oceans.* 116:C04009. doi: 10.1029/2010JC006566

Logvina, E. A., Gladysh, V. A., Kubyshkin, N. V., Nesterov, A. V., and Vinogradov, R. A. (2012). Estimation of sediment accumulation in the approach and maritime canals to the port of Sabetta (Yamal Peninsula). *Probl. Arct. Antarct.* 4, 105–118.

Makarevich, P. R. (2008). Annual successional cycle of pelagic phytocenoses in estuarine ecosystems of northern Russian seas. *Int. Algae. J.* 11, 57–63. doi: 10.1615/InterJAlgae.v11.i1.50

Makarevich, P. R., Larionov, V. V., Druzhkov, N. V., and Druzhkova, E. I. (2003). The role of phytoplankton from the Ob river in biological productivity of the Ob–Yenisei shoal. *Russ. J. Ecol.* 34, 86–90. doi: 10.1023/A:1023090812603

Miranda, L. B., Andutta, F. P., Kjerfve, B., and Filho, B. M. C. (2017). "Fundamentals of estuarine physical oceanography," in *Ocean Engineering & Oceanography*, Vol. 8, eds M. R. Dhanak and N. I. Xiros (Singapore: Springer), doi: 10.1007/978-981-10-3041-3

Moller, O. O., Castaing, P., Salomon, J. C., and Lazure, P. (2001). The influence of local and non-local forcing effects on the subtidal circulation of Patos Lagoon. *Estuaries* 24, 297–311. doi: 10.2307/1352953

Moller, O. O., Castello, J. P., and Vaz, A. C. (2009). The effect of river discharge and winds on the interannual variability of the pink shrimp Farfantepenaeus paulensis production in Patos Lagoon. *Estuar. Coasts* 32, 787–796. doi: 10.1007/s12237-009-9168-6

Monismith, S. G. (1986). An experimental study of the upwelling response of stratified reservoirs to surface shear stress. *J. Fluid Mech.* 171, 407–439. doi: 10.1017/S0022112086001507

Monteiro, P. M. S., and Largier, J. L. (1999). Thermal stratification in Saldanha Bay (South Africa) and subtidal, density-driven exchange with the coastal waters of the Benguela upwelling system. *Estuar. Coastal Shelf Sci.* 49, 877–890. doi: 10.1006/ecss.1999.0550

Nummelin, A., Ilicak, M., Li, C., and Smedsrud, L. H. (2016). Consequences of future increased Arctic runoff on Arctic Ocean stratification, circulation, and sea ice cover. *J. Geophys. Res. Oceans.* 121, 617–637. doi: 10.1002/2015JC011156

Oki, T., and Kanae, S. (2006). Global hydrological cycles and world water resources. *Science* 313, 1068–1072. doi: 10.1126/science.1128845

Olli, K., Ptacnik, R., Klais, R., and Tamminen, T. (2019). Phytoplankton species richness along coastal and estuarine salinity continua. *Am. Nat.* 194, E41–E51. doi: 10.1086/703657

Osadchiev, A. A. (2017). Spreading of the Amur river plume in the Amur Liman, the Sakhalin Gulf, and the Strait of Tartary. *Oceanology* 57, 376–382. doi: 10.1134/S0001437017020151

Osadchiev, A. A., and Korshenko, E. A. (2017). Small river plumes off the north-eastern coast of the Black Sea under average climatic and flooding discharge conditions. *Ocean Sci.* 13, 465–482. doi: 10.5194/os-13-465-2017

Osadchiev, A. A., and Sedakov, R. O. (2019). "Reconstruction of ocean surface currents using near simultaneous satellite imagery," in *Proceedings of the International Geosciences and Remote Sensing Symposium*, (Piscataway, NJ: Institute of Electrical and Electronics Engineers Inc.) 8078–8081. doi: 10.1109/IGARSS.2019.8898544

Osadchiev, A. A., Asadulin, E. E., Miroshnikov, A. Y., Zavialov, I. B., Dubinina, E. O., and Belyakova, P. A. (2019). Bottom sediments reveal inter-annual variability of interaction between the Ob and Yenisei plumes in the Kara Sea. *Sci. Rep.* 9:18642. doi: 10.1038/s41598-019-55242-3

Osadchiev, A. A., Frey, D. I., Shchuka, S. A., Tilinina, N. D., Morozov, E. G., and Zavialov, P. O. (2021a). Structure of the freshened surface layer in the Kara Sea during ice-free periods. *J. Geophys. Res. Oceans.* 126:e2020JC016486. doi: 10.1029/2020JC016486

Osadchiev, A. A., Frey, D. I., Spivak, E. A., Shchuka, S. A., Tilinina, N. D., and Semiletov, I. P. (2021b). Structure and inter-annual variability of the freshened surface layer in the Laptev and East-Siberian seas during ice-free periods. *Front. Mar. Sci.* Available online at: https://www.frontiersin.org/articles/10.3389/fmars.2021.735011/abstract

Osadchiev, A. A., Izhitskiy, A. S., Zavialov, P. O., Kremenetskiy, V. V., Polukhin, A. A., Pelevin, V. V., et al. (2017). Structure of the buoyant plume formed by Ob and Yenisei river discharge in the southern part of the Kara Sea during summer and autumn. *J. Geophys. Res. Oceans.* 122, 5916–5935. doi: 10.1002/2016JC012603

Osadchiev, A. A., Korotenko, K. A., Zavialov, P. O., Chiang, W.-S., and Liu, C.-C. (2016). Transport and bottom accumulation of fine river sediments under typhoon conditions and associated submarine landslides: case study of the Peinan River, Taiwan. *Nat. Haz. Earth Sys. Sci.* 16, 41–54. doi: 10.5194/nhess-16-41-2016

Osadchiev, A. A., Medvedev, I. P., Shchuka, S. A., Kulikov, M. E., Spivak, E. A., Pisareva, M. A., et al. (2020a). Influence of estuarine tidal mixing on structure and spatial scales of large river plumes. *Ocean Sci.* 16, 1–18. doi: 10.5194/os-16-1-2020

Osadchiev, A. A., Pisareva, M. N., Spivak, E. A., Shchuka, S. A., and Semiletov, I. P. (2020b). Freshwater transport between the Kara, Laptev, and East-Siberian seas. *Sci. Rep.* 10:13041. doi: 10.1038/s41598-020-70096-w

Osadchiev, A. A., Silvestrova, K. P., and Myslenkov, S. A. (2020c). Wind-driven coastal upwelling near large river deltas in the Laptev and East-Siberian seas. *Remote Sens.* 12:844. doi: 10.3390/rs12050844

Pavlov, V. K., Timokhov, L. A., Baskakov, G. A., Kulakov, M. Y., Kurazhov, V. K., Pavlov, P. V., et al. (1996). *Hydrometeorological regime of the Kara, Laptev, and East-Siberian seas.* Technical Memorandum, APL-UW TM 1-96, Applied Physics Laboratory. Washington: University of Washington.

Pogojeva, M., Zhdanov, I., Berezina, A., Lapenkov, A., Kosmach, D., Osadchiev, A., et al. (2021). Distribution of floating marine macro-litter in relation to oceanographic characteristics in the Russian Arctic seas. *Mar. Poll. Bull.* 166:112201. doi: 10.1016/j.marpolbul.2021.112201

Polukhin, A. (2019). The role of river runoff in the Kara Sea surface layer acidification and carbonate system changes. *Environ. Res. Lett.* 14:105007. doi: 10.1088/1748-9326/ab421e

Stigebrandt, A. (1990). On the response of the horizontal mean vertical density distribution in a fjord to low-frequency density fluctuations in the coastal water. *Tellus Ser. A* 42, 605–614. doi: 10.3402/tellusa.v42i5.11902

Sukhanova, I. N., Flint, M. V., Sakharova, E. G., Fedorov, A. V., Makkaveev, P. N., and Nedospasov, A. A. (2018). Phytocenoses of the Ob estuary and Kara Sea shelf in the late spring season. *Oceanology* 58, 802–816. doi: 10.1134/S0001437018060139

Sukhanova, I. N., Flint, V. M., Mosharov, S. A., and Sergeeva, V. M. (2010). Structure of the phytoplankton communities and primary production in the Ob River estuary and over the adjacent Kara Sea shelf. *Oceanology* 50, 743–758. doi: 10.1134/S0001437010050115

Voinov, G. N. (2016). Tides in the Gulf of Ob (Kara Sea). I. General characteristics of tide. *Sci. Notes RSHU* 44, 70–95.

Vvedensky, A. R., Diansky, N. A., Kabatchenko, I. M., Litvinenko, G. I., Reznikov, M. V., and Fomin, V. V. (2017). Calculation and analysis of the expected impact of the hydrotechnical construction on the environmental condition in the water area and bottom topography in case of the construction of the approach channel to the Sabetta Port. *Vestn. MGSU* 12, 480–489. doi: 10.22227/1997-0935.2017.5.480-489

Yakushev, E., Gebruk, A., Osadchiev, A, Pakhomova, S., Lusher, A., Berezina, A., et al. (2021). Microplastics distribution in the Eurasian Arctic is affected by Atlantic waters and Siberian rivers. *Comm. Earth Environ.* 2:23. doi: 10.1038/s43247-021-00091-0

Zavialov, I. B., Osadchiev, A. A., Sedakov, R. O., Barnier, B., Molines, J.-M., and Belokopytov, V. N. (2020). Water exchange between the Sea of Azov and the Black Sea through the Kerch Strait. *Ocean Sci.* 16, 15–30. doi: 10.5194/os-16-15-2020

Conflict of Interest: The authors declare that the research was conducted in the absence of any commercial or financial relationships that could be construed as a potential conflict of interest.

Publisher's Note: All claims expressed in this article are solely those of the authors and do not necessarily represent those of their affiliated organizations, or those of the publisher, the editors and the reviewers. Any product that may be evaluated in this article, or claim that may be made by its manufacturer, is not guaranteed or endorsed by the publisher.